Application of spectral decomposition to gas basins in Mexico

MICHAEL DEAN BURNETT and JOHN PATRICK CASTAGNA, Fusion Geophysical, Norman, Oklahoma, U.S.
EFRAÍN MÉNDEZ-HERNÁNDEZ, GENARO ZIGA RODRÍGUEZ, LEONEL FIGÓN GARCÍA, JOSÉ TRINIDAD MARTÍNEZ VÁZQUEZ, MARIANO TÉLLEZ AVILÉS, and RAÚL VILA VILLASEÑOR, Petróleos Mexicanos, Ciudad Pemex, Mexico

Recent reservoir studies involving spectral decomposition on various data sets from the Burgos and Macuspana basins of Mexico document the usefulness of this method as another way to uncover the effects of hydrocarbon accumulations on seismic data. Three such effects are illustrated in this article; attenuation of seismic waves passing through the reservoir, preferential reservoir illumination, and differential reservoir reflectivity.

Such phenomena can be clearly seen in these seismic studies only because of the use of a new method of spectral decomposition, the wavelet transform. Traditionally, spectral decomposition has used various techniques that require the use of a time window (e.g. Fast Fourier transform, discrete Fourier transform, maximum entropy, etc.). These windows produce serious distortion of true spectra and/or severely limit the vertical resolution; discrete spectral energy from individual reflection events that fall inside the window are mixed together, and when the window length is shortened to minimize this problem, frequency discrimination is compromised. Wavelet transforms, on the other hand, have no such windowing requirements and therefore avoid this distortion. Note that spectral decomposition, like inversion, is nonunique, but the wavelet transform generally does a vastly superior job of representing the individual wavelet spectra than windowed methods. This is the primary reason why analyses using the traditional techniques have been limited to map extractions. The windowed techniques do not preserve the individual reflection events and introduce distortions and artifacts. The ability to analyze the spectra of individual reflections is a major leap forward in the effectiveness of spectral decomposition.

Burgos Basin studies. Two studies in northeastern Mexico illustrate the phenomena of differential reservoir reflectivity and attenuation of seismic waves passing through the reservoir. Figure 1 shows the location of Burgos Basin and Alondra and Numerador fields. Alondra produces from clean Midway-age sands with thickness of approximately 20 m and with porosities of
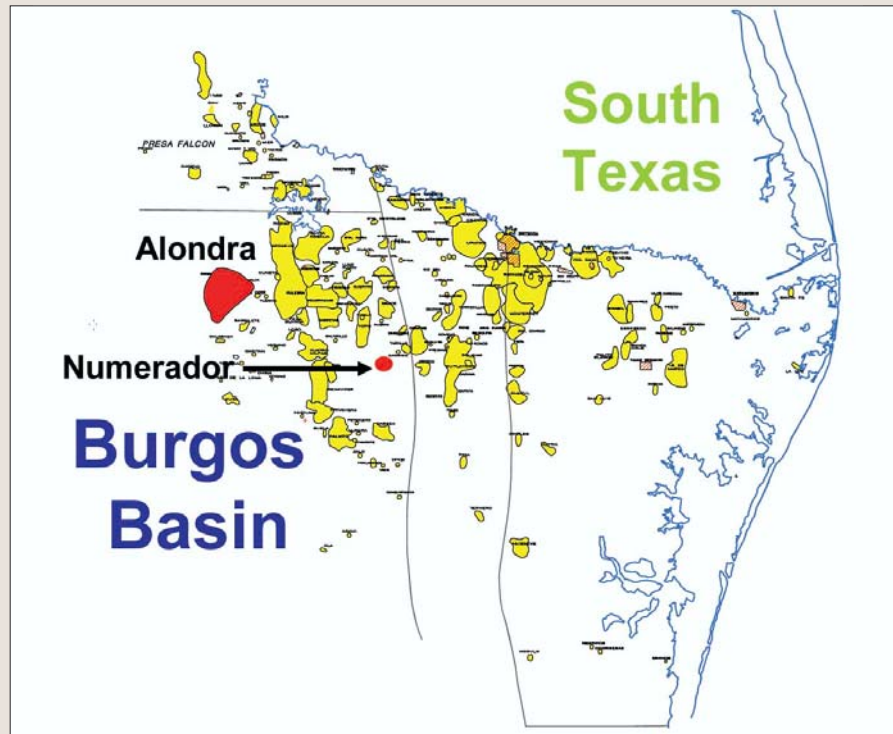

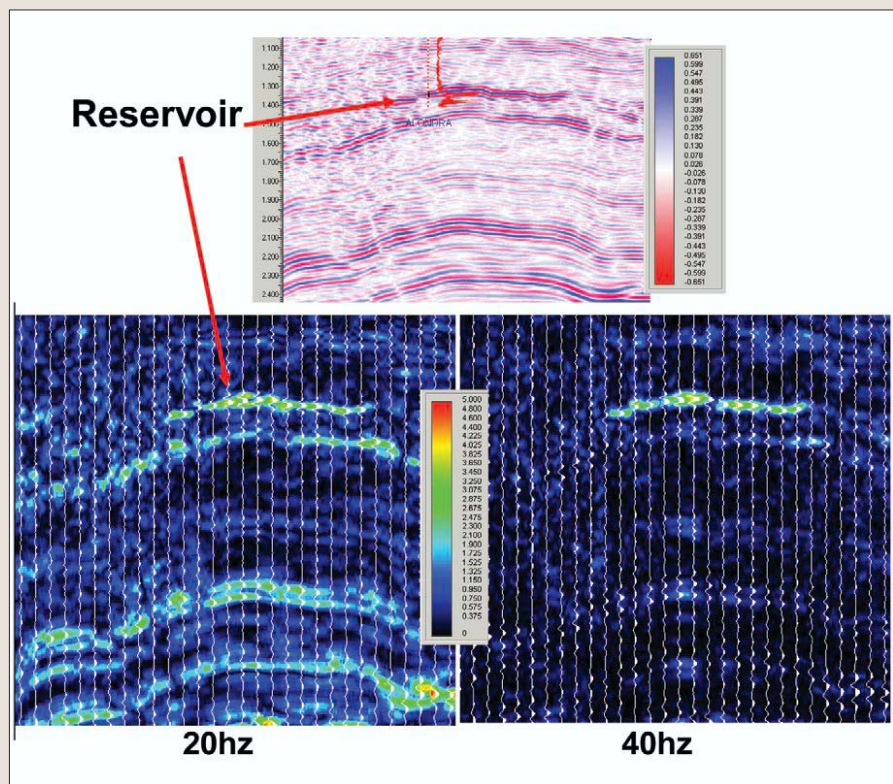*Figure 1.* The Burgos Basin and the locations of Alondra and Numerador studies.

Figure 2. Midway gas reservoir showing differential reflectivity. The reservoir is not anomalous at 20 Hz but exhibits anomalous reflectivity at 40 Hz.
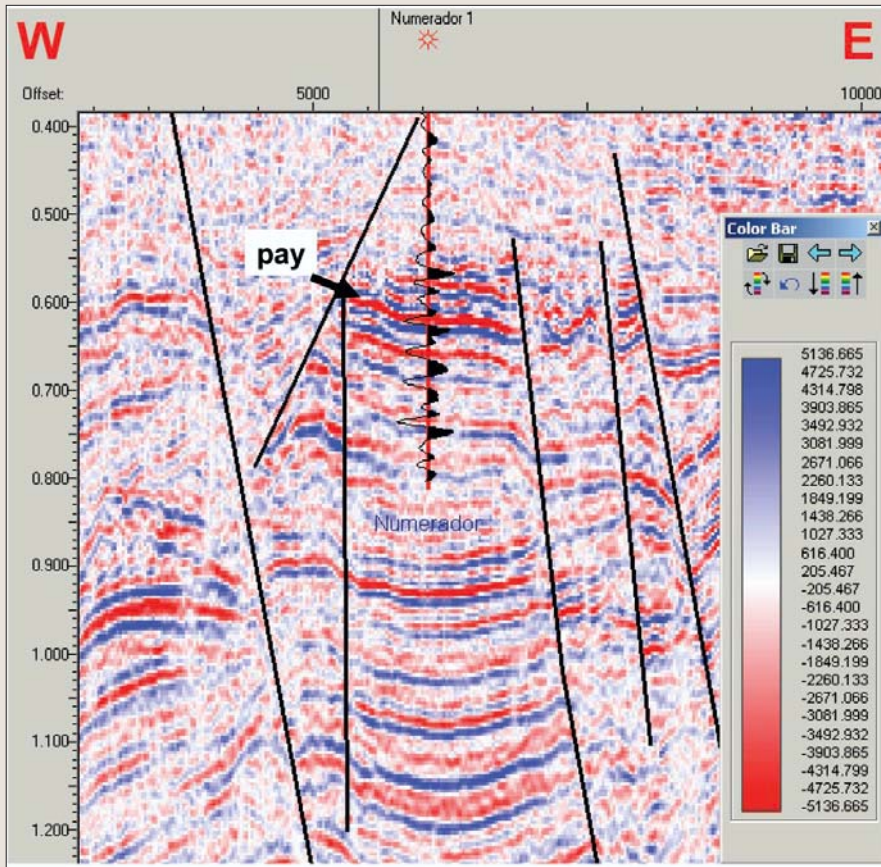
Figure 3. Arbitrary line across Numerador Field showing a gas accumulation in a shallow Jackson sandstone.

13-18% (low impedance) at a depth of approximately 2000 m. Figure 2 shows two isofrequency panels and the inline used as input. At 20 Hz the reservoir does not exhibit an anomalous reflectivity compared with the surrounding geology. But at 40 Hz, the gas charged sand clearly stands out. This behavior can be partially explained by the fact that the time-thickness of this sand is close to tuning; it will appear as a dipole. When filled with gas, the reflectivity of the sand is higher and the amplitude at all frequencies is increased over the adjacent brine-filled geology and the center frequency of the reflection from the reservoir is increased slightly. This same effect can be duplicated in synthetic models constructed using local well logs.

This effect becomes spectacular when viewed in frequency maps as that from Numerador Field (Figure 3). The discovery well produces gas from a high porosity, low-impedance Jackson sandstone which is 17 m thick at a depth of 500 m. This field is trapped to the south and southwest by a prominent fault and by dip to the north and east. The line in Figure 3 crosses the Numerador well. The sands here are locally conformable and the phenomena of attenuation can be demonstrated with this reservoir.
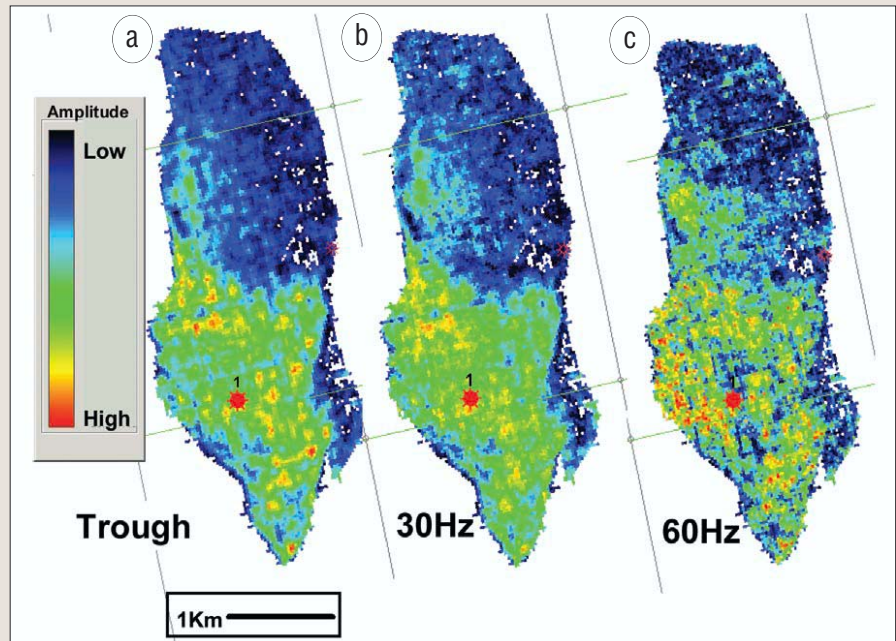
Figure 4. *(a) Standard amplitude map of pay. (b) 30-Hz frequency map. (c) 60-Hz frequency map. Note the subtle differences between the frequency maps, especially the hole in amplitude immediately north of the Numerador at 50 Hz. This hole is probably due to a local thickening of the reservoir.*
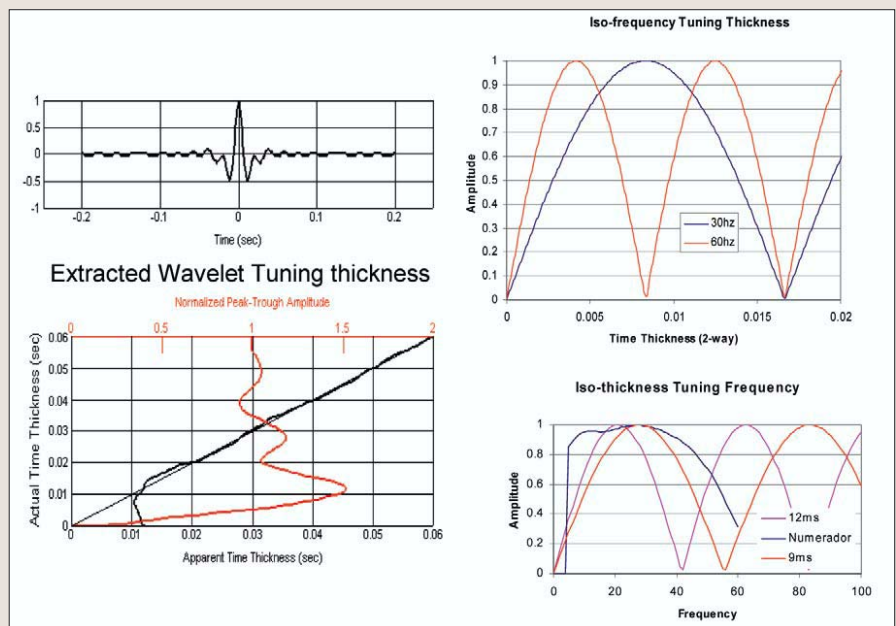

Figure 5. *Tuning chart for extracted wavelet and individual frequencies at 30 Hz and 60 Hz versus theoretical tuning frequencies and observed spectral behavior at Numerador. Compare these to the maps in Figure 4.*

Since this gas accumulation can be obviously identified via an amplitude map, it is instructive to compare the full-spectrum conventional amplitude map with its equivalent at discrete frequencies. Figure 4 shows the reservoir fault block map of conventional amplitudes of the trough after residual phase removal, along with two frequency maps of the same horizon. Spectral stabilization has been applied to remove the wavelet spectra from these maps; without this step, overall map ampli-tudes between frequencies are dominated by wavelet spectra and discerning true spectral behavior of the geology is difficult.

Attention is directed toward the area immediately north of the Numerador well. While both the conventional amplitude map and the frequency maps reveal the reservoir's orientation, the frequency maps show a different distribution of amplitudes within the reservoir. One reason for this might be reservoir thickness.
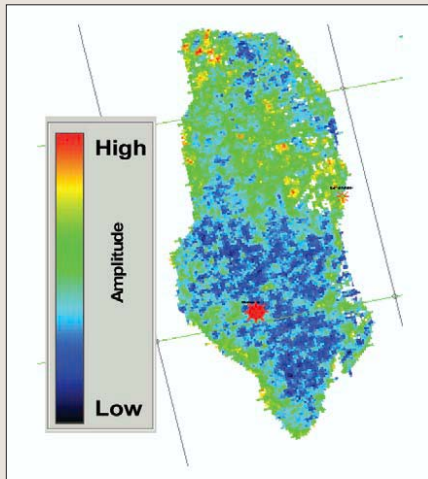
Figure 6. *Average amplitudes under the reservoir at 20 Hz.*

In order to investigate this possibility, Figure 5 contains the full wavelet tuning characteristics and those of the individual frequencies shown in Figure 4, along with the theoretical tuning frequency chart for a reflector with thickness equal to that observed at Numerador. The apparent seismic time thickness at the Numerador well (trough-peak) is about 12 ms (close to maximum tuning for the full-spectrum wavelet); theoretical maximum amplitude for this thickness should occur at about 21 Hz. Observed amplitudes at each frequency were extracted from the maps at Numerador and then normalized and plotted to compare with expected results. This curve shows that maximum amplitude at Numerador occurs at about 28 Hz. The rate of amplitude decay above that frequency does not match the expected spectral behavior from this known reservoir thickness. Therefore, other factors are also contributing to the spectral behavior of these data. In all three maps, for instance, acquisition/processing artifacts can clearly be observed. Most importantly, however, the reservoir is not a simple isolated layer as assumed in the tuning charts. Variable reflectivity structures require more sophisticated methods for thickness determination. Thus, the spectral behavior is due to a combination of factors at Numerador. Work continues on this example to try to better understand these results. Such investigations are impossible with techniques that use windows in the calculations.

Figure 6 shows a map of average amplitudes in a 50-ms window approximately 10 ms below the reservoir at 20 Hz. This low amplitude (which is also present at all other frequencies) is evidence of the attenuation of the reser-
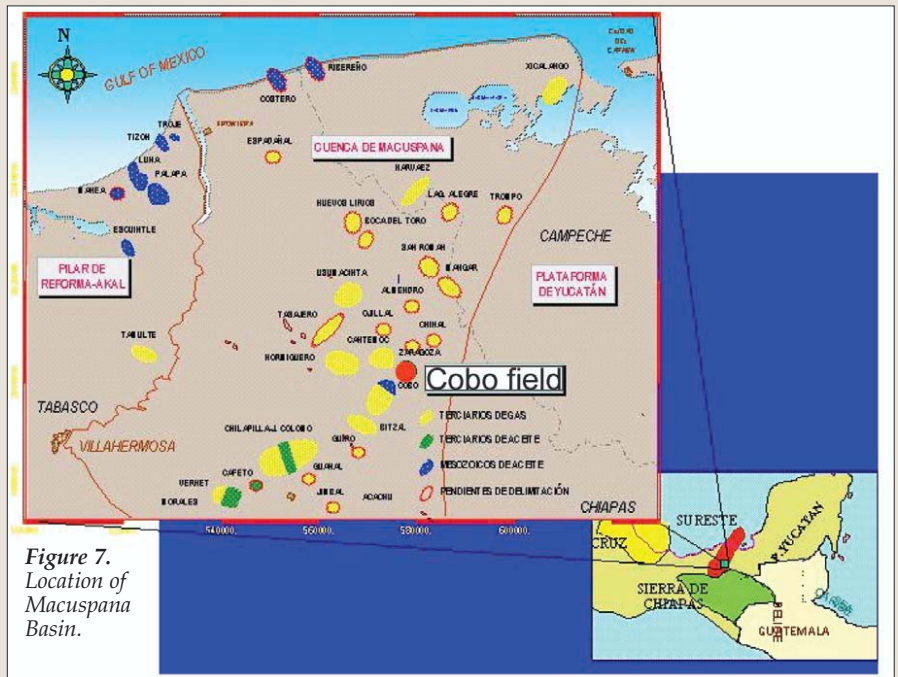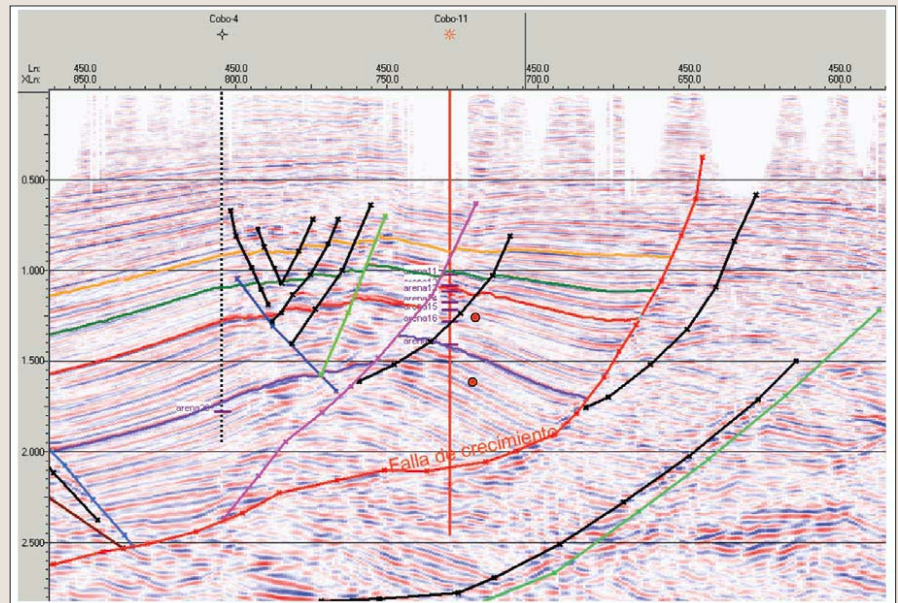

Figure 7. *Location of Macuspana Basin.*

Figure 8. *Seismic section showing structural/stratigraphic features of the Cobo/Bitzal area.*
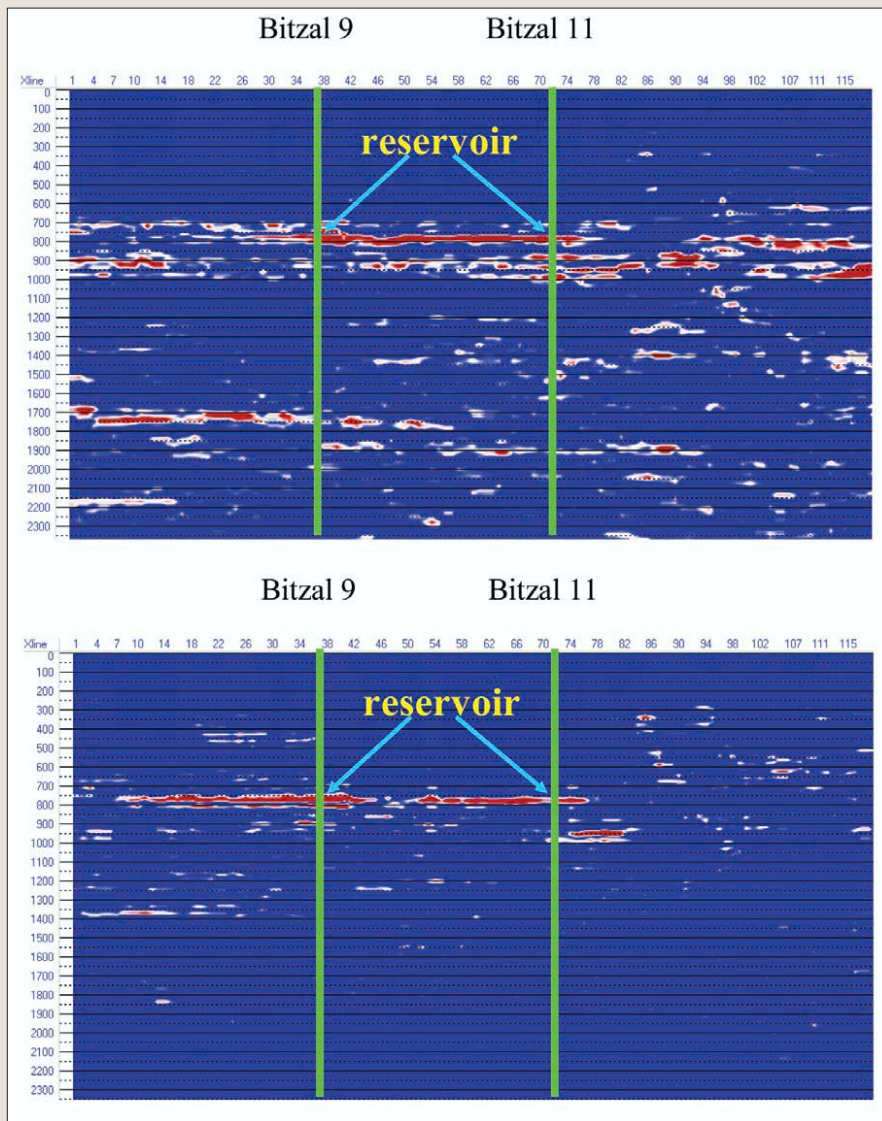
Figure 9. *Isofrequency panels showing the reservoir to be more anomalous and resolved better at 35 Hz (bottom) than at 25 Hz (top); the reservoir pressures in the two wells are different. Notice in particular how much farther to the left than the reservoir extends on the 35-Hz section.*

continuous, with reservoir pressure and water levels indicating complex reservoir geometry (Figure 8). Spectral decomposition was successfully used here to indicate lateral heterogeneity. Figure 9 shows two isofrequency panels with the reservoir indicated. The reservoir appears continuous on the 25-Hz panel but is discontinuous on the 35-Hz panel. In fact, the reservoir has a different pressure in these two wells, indicating that the discontinuity evident only on the 35-Hz panel is likely to be real. Bitzal 11 is now plugged but Bitzal 9 is still producing. The fact that the reservoir amplitude extends further to the left on the 35-Hz panel suggests that the reservoir is thinning in that direction. The idea here is that the gas in the reservoir changes the resonant frequency (shifting this frequency upward as shown in the first example). This makes the reservoir (and gaps between sand bodies) easier to see when illuminated at the resonant frequency. This type of analysis would not be possible without the ability to resolve individual reflection events, as the wavelet transform allows us to do.

Conclusion. We have shown examples of spectral decomposition using wavelet transforms applied to problems in two basins in Mexico. This technique has been shown to be a valuable aid in the search for hydrocarbons in these gas-prone areas as in the direct detection of hydrocarbons and as an indicator of stratigraphic variability. T|E

Corresponding author: mburnett@fusiongeo.com

voir of seismic waves passing through the gas column. Note that the low-amplitude area corresponds to the high-amplitude area in Figure 4 and is consequently interpreted to be caused by gas-related attenuation or transmission loss.

Macuspana Basin example. Figure 7 shows that Macuspana Basin is just southwest of the Yucatan peninsula. Production here is from thin Plio-Plistocene sands thought to be fluvial in origin. These sands can be quite dis-